Available online at www.sciencedirect.com
SCIENCE DIRECT®
Journal of Fluorine Chemistry 125 (2004) 1087–1094
JOURNAL OF FLUORINE CHEMISTRY
www.elsevier.com/locate/fluor

Optimization of HDPE direct fluorination conditions by XPS studies

Ana Maria Ferraria, José Dias Lopes da Silva, Ana Maria Botelho do Rego*

IST, Centro de Química-Física Molecular, Complexo Interdisciplinar, Av. Rovisco Pais, 1049-001 Lisbon, Portugal

Received 12 November 2003; received in revised form 14 January 2004; accepted 18 January 2004

Available online 26 February 2004

Abstract

A fluorination reactor was designed and built in the laboratory. The optimal conditions of fluorination within the reactor were selected by X-ray photoelectron spectroscopy (XPS) and scanning electron microscopy (SEM) analysis of fluorinated surfaces of a film and a plaque of pure high-density polyethylene (HDPE). This reactor was used to post-mould fluorinate plaques and films of a range of mixtures of virgin and recycled HDPE with and without (re)introduction of additives. The ability to be fluorinated has shown no dependence on the composition virgin/recycled HDPE.

Comparison of in-line and post-mould fluorinated samples showed that fluorine concentration profile in depth is thinner in the in-line fluorinated sample when compared with the post-mould fluorinated sample, though the fluorination degree in the extreme surface is larger in the in-line fluorinated sample. This is attributed to a migration of lower surface energy chain blocks towards the surface in the material at high temperatures, which is the case in the in-line fluorination, hindered in the post-mould fluorination where maximum temperature is below the melting point to keep the macroscopic shape. The additives played a minor role in the ability of the surface to be fluorinated.

Keywords: HDPE surface; HDPE recyclate; Direct fluorination; XPS

1. Introduction

The low and selective permeability of polymers to many fluids, gaseous or liquids, is of great importance in a great number of applications, such as packaging films, electrical cables, textiles, protecting clothes, fuel tanks, membranes, etc. Fluorocarbon resins are very well known polymers having just that property.

In many applications, however, there is a need to combine a high hydrophobicity and oleophobicity with bulk mechanical and rheological properties different from the ones in fluororesins. One of the solutions, in many applications, is to fluorinate just the polymer surface. Among the methods of surface fluorination usually reported in literature, we can cite treatment in a carbon tetrafluoride (CF_4) plasma [1,2], segregation to the surface of especially designed fluorinated molecules [3] and direct fluorination achieved by using a flow of fluorine gas (F_2), pure or diluted into an inert gas, impinging on the surface [4]. A specific example of this last method is used in the European plastic fuel tank industry where the low permeability to hydrocarbons and the other main components of fuel is assured by the fluorination of the inner walls of the tanks and will be here called ''in-line'' fluorination [5]. For this case, the direct fluorination is made during the blowing of the tank, i.e. at high temperature. For ''post-mould'' direct fluorination, i.e. fluorination of a piece of plastic after moulding, some designs of reactors are reported in the literature [6]. This kind of fluorination has many industrial applications and can be particularly useful in laboratory conditions to understand the role of all the components of the polymer (namely the additives) on the quality of the fluorination layer, thickness, homogeneity and amount of fluorine. This is particularly useful in the case of the increasing use of HDPE recyclate from fuel tanks where the evaluation of the *fluorability* (ability to be fluorinated) of the recycled material compared with the virgin material is an important parameter to decide whether reuse in the same application is possible.

Many techniques are used to study the composition and properties of the fluorinated layer [7].

One of the most powerful, given its specificity to the surface, is X-ray photoelectron spectroscopy (XPS). With its capability to make qualitative and quantitative elemental analysis and to detect the chemical environment of each element through the ''chemical shift'', it can provide very complete chemical information about the 10–20 first layers of a flat surface.

* Corresponding author. Tel.: +351-21-8419255/7; fax: +351-21-8464455/7.
E-mail address: amrego@ist.utl.pt (A.M. Botelho do Rego).

0022-1139/$ – see front matter © 2004 Elsevier B.V. All rights reserved.
doi:10.1016/j.jfluchem.2004.01.014

One of the limitations of XPS is the degradation that X-rays may induce in organic materials especially in halogenated species, as is the case in fluorinated surfaces. This limitation may be important in the case where information about the elemental concentration as a function of depth is needed. Another problem associated with XPS analysis of polymer surfaces originates from the low electrical conductivity of samples, leading to surface charging. These two problems were thoroughly discussed elsewhere and solutions were presented to minimize them [8].

The action of fluorine on the surface topography must also be considered. Pitting phenomena induced by direct fluorination have been reported [9]. This implies that the analysis of the topography of the surface by scanning electron microscopy (SEM) is very important to ensure that the surface is uniform after fluorination.

In this work, we present a study of polyethylene surfaces, modified by direct fluorination, using X-ray photoelectron spectroscopy and scanning electron microscopy. XPS data are treated in an original way according to a methodology presented elsewhere [8], which provides a good way of assigning XPS C1s components even if the absolute binding energies cannot be determined.

2. Results and discussion

2.1. Selection of fluorination conditions

In order to choose effective conditions for laboratory fluorination, tests with a film of pure HDPE provided by Solvay were performed. Varying parameters were fluorine content in gaseous flow (from 0.013% (v/v) to 0.09% (v/v)), time of exposure (from 5 to 20 min) and temperature (from room temperature to 97 °C).

The extent of the fluorination was assessed by XPS, measuring the global F/C atomic ratio computed from the F1s and C1s peak areas and also the F/C atomic ratio computed from the C1s region [8]. The ratio between these two parameters, here called F/C ratio, gives a qualitative indication of typical dimensions of fluorine density depth profile. XPS peak fitting, was performed using Voigt profiles 50% lorentzian. For C1s region, full width at half maximum (FWHM) was constrained to be the same for all the components. The value obtained for FWHM in the samples here presented was around 2 eV. For the F1s region, a peak ~2.4 eV wide was fitted for all the samples. In Fig. 1, XPS C1s and F1s spectra for two different samples are shown as an example. EF3 was fluorinated for 5 min at a temperature of 47 °C with a gaseous flux containing dry nitrogen and 0.02% (v/v) of fluorine ($[F_2] = 0.02\%$) and EF19 was fluorinated for 20 min at a temperature of 97 °C with $[F_2] = 0.064\%$.

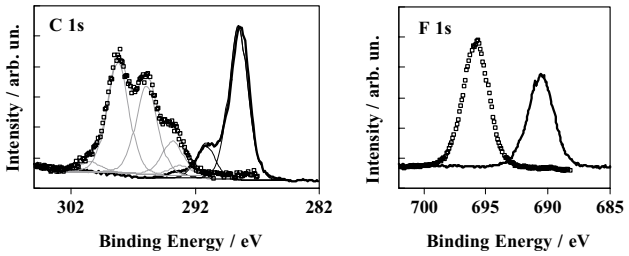

Fig. 1. XPS C1s and F1s spectra for two samples: (—) one fluorinated for 5 min with $[F_2] = 0.02\%$ (v/v) and 47 °C (sample EF3); (□) another one fluorinated for 20 min with a $[F_2] = 0.064\%$ (v/v) and ~97 °C (sample EF19). Fitted components to C1s region are shown in grey for EF 19 sample and in black for EF 3 sample. Binding energies are not corrected for charging effects. Spectra were normalized to the same baseline. C1s region for pure virgin HDPE is not shown for figure clarity sake but it has a single peak [10].

The peak fitting to regions F1s and C1s yields parameters contained in Table 1.

In sample EF3, the charging shift is easy to compute since the most part of the carbon is bound to CH_2 far from the fluorine neighbourhood and we can attribute to it the binding energy of 285 eV [10]. We can, then, identify two peaks corresponding to carbon bound to fluorine: one 2.7 eV shifted from the CH_2 peak (at 287.7 eV) and the other

Table 1
Peak assignment and area % for C1s peak for samples in Fig. 1

	EF3 ($t_F = 5$ min; $[F_2] = 0.02$ vol.%; $T = 47$ °C)		EF19 ($t_F = 20$ min; $[F_2] = 0.064$ vol.%; $T = 97$ °C)	
	ΔBE* (eV)	Area %	ΔBE* (eV)	Area %
CH_2 (in a fluorine poor neighbourhood)	402.2	79.6	402.5	3.9
CH_2 (in a fluorine rich neighbourhood)			401.9	14.2
CF	399.5	17.1	399.8	35.0
CF_2	397.2	3.3	397.5	43.2
CF_3			395.2	3.7
Global F/C	0.28		1.54	
F/C (C1s)	0.24		1.33	
F/C ratio**	1.16 ± 0.05		1.17 ± 0.05	

Global F/C atomic ratios and F/C computed from C1s region as well as their ratio, are also presented.
* $\Delta BE = BE_{F1s} - BE_{C1s}$.
** F/C ratio = (global F/C)/(F/C (C1s)).

5 eV shifted (at 290 eV). Their identification is based on BE differences between F1s and C1s peaks [8], the first corresponds to CF groups and the second one to CF_2 groups. Both Fig. 1 and Table 1 show that the sample exposed to a flux richer in fluorine (sample EF19) has a more extensively fluorinated surface as shown by the global F/C ratio and by the atomic percentage of fluorinated carbons. The F/C ratio = (global F/C)/(F/C (C1s)) is also included. As shown in reference [8] its deviation from unity gives an indication of the existence of a fluorine profile decreasing with depth, having a typical dimension, l, <100 Å. In fact, for an exponential schematic profile for fluorine density ($n_F \propto \exp(-x/l)$, n_F being the bound fluorine density in depth), a flat surface and assuming a constant carbon density, we have Eq. (1), [8]:

$$\text{F/C ratio} = \frac{\text{F/C}}{\text{F/C(C 1s)}} = \frac{\lambda_C + l}{\lambda_F + l} \quad (1)$$

where $\lambda_C = 31.2$ Å and $\lambda_F = 20.5$ Å are the effective attenuation length of the C1s and F1s photoelectrons, respectively. This shows that if $l \gg l_C$ that ratio tends to 1 and when $l \to 0$, F/C ratio approaches 1.52.

Values obtained in Table 1 show that for these two films, the fluorinated layer is rather homogeneous and thicknesses are very similar. If the assumptions about the fluorine density profile shape and the flatness of the surface are correct, it appears that the typical dimension of the fluorinated layer ranges from 30 to 70 Å.

In Fig. 2, the global F/C ratios obtained by XPS as a function of temperature, F_2 contents on the flow, and time are shown.

It can be concluded that the extent of the fluorination is greater for higher temperatures but it seems to attain a plateau around 85 °C. It must be noted that, with this kind of sample (HDPE film) and this type of reactor, the study is limited to a maximum temperature of ~100 °C due to the melting point of this material (132 °C [11]) and to the highly exothermic character of the fluorination reaction ($\Delta H_r = -399$ kJ mol^{-1} [12]). We verified that for a fluorine content in the flow entering the reactor, [F_2], below 0.02% (v/v), for a time of fluorination, t_F, below 15 min and for a temperature of the reactor ≤50 °C, the global F/C atomic ratio is <1. This ratio rises for longer times of exposure to the gaseous flow, higher temperatures and higher concentrations of F_2. Fixing the time parameter at 20 min and increasing [F_2], it was possible to obtain a global F/C ratio near 1.6, with [F_2] = 0.064% (v/v) at 97 °C. The optimisation of experimental conditions was recalibrated for commercial samples from CIBA. These samples were in the form of plaques, allowing analysis in a larger temperature range, up to ~115 °C. The study of the influence of [F_2] on the extent

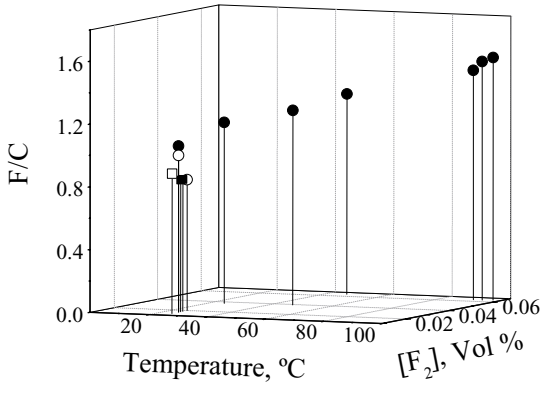

Fig. 2. Evolution of the relative amount of fluorine with three experimental parameters: the reactor's temperature, the fluorine gaseous concentration entering the reactor and the time of fluorination (□) 5 min; (■) 10 min; (○) 15 min; (●) 20 min.

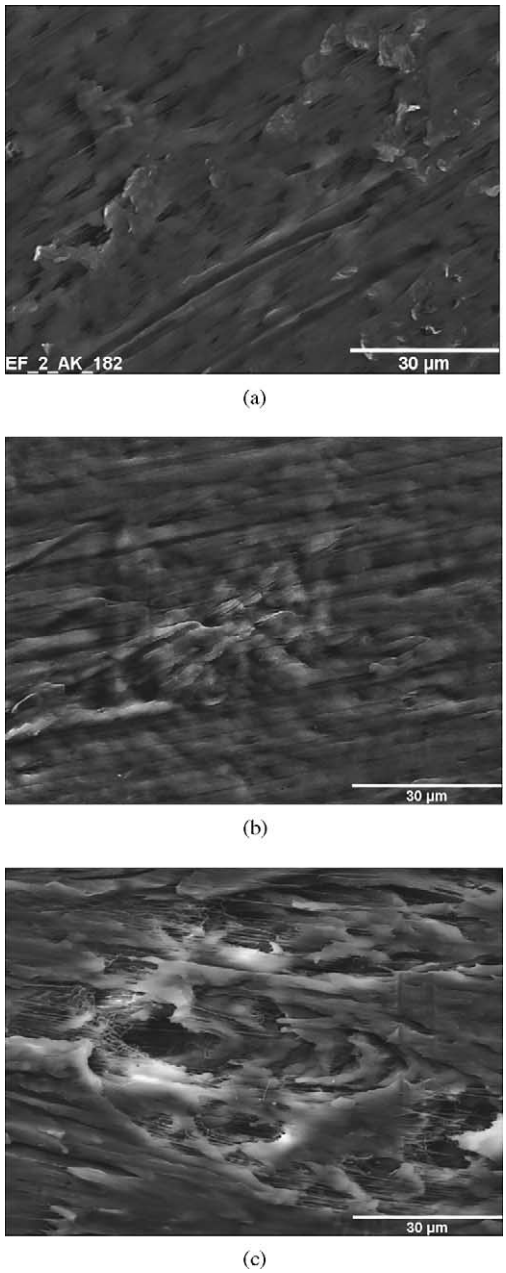

(a)

(b)

(c)

Fig. 3. SEM images for three plaques post-mould fluorinated for 20 min at 90 °C, with [F_2] volume percentages of (a) 0.06; (b) 0.08; (c) 0.09.

of the fluorination was limited to the contents of fluorine in the mixture ($N_2 + F_2$) we used (0.09% (v/v)). With $[F_2] = 0.09\%$ (v/v) a F/C ratio 10% higher than with 0.06% (v/v) was obtained. However, a fluorine gaseous concentration that did not exceed 0.065% (v/v) was chosen. In fact, the images obtained by SEM (Fig. 3) of three samples, fluorinated with an increasing content of F_2: 0.06, 0.08 and 0.09% (v/v), show that the surfaces are severely damaged, showing some pitting effect or even melted zones. These topographic changes become more evident for higher $[F_2]$. For that reason, a limit around 0.06% (v/v) was established, in order to keep some uniformity after the surface treatment together with a good degree of fluorination.

This large effect of fluorination on surface topography, led to analysis by SEM of two samples with the same base composition, the same surface treatment, before and after X-ray irradiation. The result is shown in Fig. 4 for two fluorinated samples at ~90 °C, for 20 min and $[F_2] = 0.06\%$ (v/v).

Images in Fig. 4 were obtained from two different pieces of a same sample, since after SEM analysis, due to the gold coating on the surface, the same piece of the sample cannot be analysed by XPS. Therefore, for the X-ray doses here used, the similarity of the images shows that the chemical degradation of the surface, already shown in reference [8], is not accompanied by a topographic degradation in spite of the release of F_2 and/or HF from the surface during irradiation. It was also verified that the central portion of the sample (placed at the centre of the reactor) was less fluorinated than the peripheral regions. In what follows the peripheral regions are compared. From this study, the following conditions of fluorination were used for the "real" samples: $T = 95$–105 °C; $[F_2] = 0.064 \pm 0.002\%$ (v/v); $t_F = 20$ min.

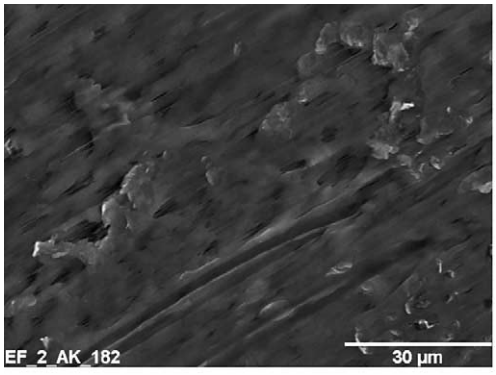

(a)

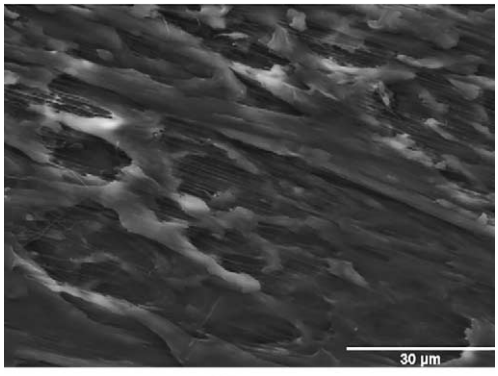

(b)

Fig. 4. SEM images for two post-mould fluorinated samples at ~90 °C, for 20 min at $[F_2] = 0.06\%$ (v/v) (a) before X-ray irradiation; (b) after X-ray irradiation for 120 min.

2.2. Correlation between resin formulation and surface fluorination ability

The characteristics of a fluorinated layer depend on the fluorination method itself, on the chemical structure of the polymer and on the possible reintroduction of additives needed to restore the chemical, mechanical and/or rheological properties of a polymer at the end of its lifecycle. In order to evaluate the ability of samples with different amounts of recycled material to be fluorinated, samples were fluorinated under the same laboratory conditions ($T = 75 \pm 2$ °C; $[F_2] = 0.062 \pm 0.002\%$ (v/v); $t_F = 20 \pm 1$ min) and analysed by XPS. To ensure that the fluorination conditions were exactly the same for all the samples, they were placed in a circle around the centre of the reactor, fluorinated simultaneously, and then kept under nitrogen atmosphere prior to analysis. Samples, under the form of plaques were mixtures of virgin HDPE without any additive and HDPE recyclate with an additive (0.5% (w/w) of Recycloblend™, an additive from CIBA). Compositions ranged from 100% virgin HDPE to 100% HDPE recyclate.

The elemental quantitative analysis of C1s and F1s regions acquired at a take-off-angle relative to the surface (TOA) of 90° shows that, within the experimental error, the relative amount of fluorine does not change with the amount of recycled material present in the sample (Fig. 5).

The average global F/C is around 1.46 and average F/C (C1s) is 1.34. The average value for F/C ratio is therefore, 1.1. All these values are close to the optimal obtained for virgin HDPE films at the same temperature, time and $[F_2]$.

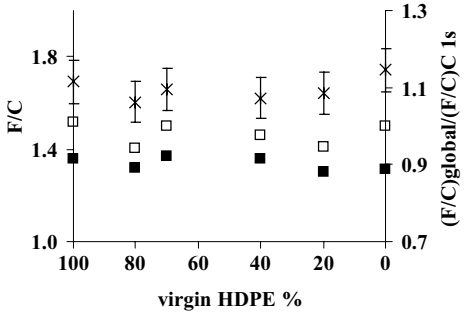

Fig. 5. Relative amount of fluorine in samples with different % of virgin HDPE: (□) global F/C atomic ratio; (■) F/C ratio computed from C1s region; (⨯) F/C ratio (defined in the text).

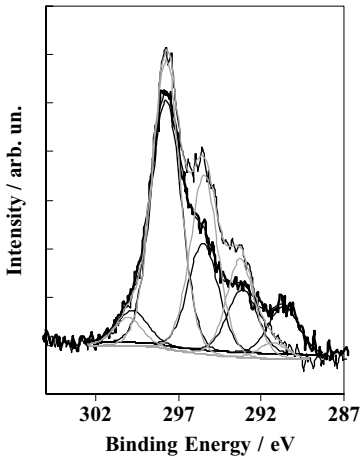

Fig. 6. XPS C1s region for a sample fluorinated in-line (bold line) and another "post-mould" fluorinated (thin line). Fitted components are in black for the in-line sample and in grey for the post-mould-one. Binding energy was not corrected for charging effects. Spectra were normalized to the same baseline.

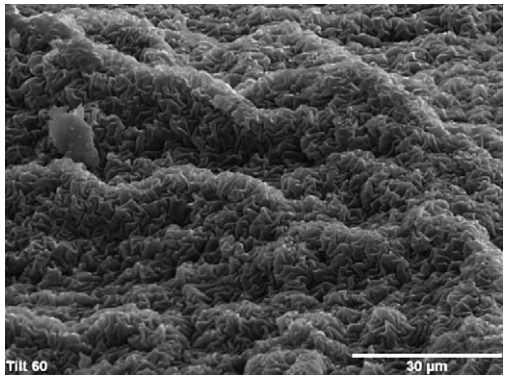

Fig. 7. SEM image of an in-line fluorinated sample.

2.3. Post-mould versus in-line fluorination

The elemental analysis of the samples treated by post-mould fluorination and the analysis of the samples fluorinated "in-line" indicated that the F/C ratio was always larger in the latter ones but the nature of the fluorinated groups was essentially the same as can be seen in Fig. 6 and Table 2.

The global F/C is different in the two samples though the F/C (C1s) is the same. This yields different F/C ratios, the distance from unity being larger in the in-line fluorinated sample. This means that the fluorine composition is less uniform in depth than in the post-mould sample. A possible explanation is as follows: though the diffusion of fluorine is larger in the in-line fluorination because the HDPE is a melt, the diffusion of the lower energy surface components towards the extreme surface is also larger. The result is a fluorine concentration profile less uniform, richer in fluorine at the extreme surface of the in-line fluorinated sample, but also a much more wrinkled surface as shown by SEM in Fig. 7.

With such a rough surface, it is impossible to perform angle resolved X-ray photoelectron spectroscopy (ARXPS) studies to obtain further information about the fluorine concentration profile. The segregation of the lower energy surface components explains also why the in-line fluorinated sample is richer in (CF_2)-groups than the post-mould.

Another difference between the two samples arises from the peak at low binding energy; in the in-line sample it is 404.5 eV from the F1s peak whereas in the post-mould it is 403.9 eV. This means that the lower binding energy C1s peak is 0.6 eV lower in the in-line fluorinated sample than in the post-mould. This means that, in the in-line sample, that peak corresponds to unreacted carbon black (BE = 284.4 eV), which migrates towards the surface before the sample cools. Apparently, in the post-mould fluorination, the surfacial carbon black reacts with fluorine and the temperature within the reactor is not high enough to allow for the migration of unreacted carbon black towards the surface. Degradation studies of the in-line fluorinated sample show that the peak at 284.4 eV disappears with the degradation by X-ray irradiation. This could be due to a reaction of the remaining surfacial carbon black with the fluorine and hydrogen resulting from the degradation. Since the F1s peak always shows just one component, fluorine binds mainly covalently to sp^3 atoms in the carbon black. Therefore, respective spectra, both in C1s and F1s regions,

Table 2
Peak assignment and area % for C1s peak for samples in Fig. 6

	In-line		Post-mould	
	ΔBE (eV)	Area %	ΔBE (eV)	Area %
CH_2 (in a fluorine poor neighbourhood)	404.5	9.6	403.9	2.5
CH_2 (in a fluorine rich neighbourhood)	402.0	12.7	402.0	16.1
CF	399.6	21.6	399.8	29.3
CF_2	397.4	49.6	397.5	47.4
CF_3	395.3	6.4	395.2	4.6
Global F/C	1.73		1.52	
F/C (C1s)	1.40		1.38	
F/C ratio	1.24 ± 0.05		1.10 ± 0.05	
CF_2/CF	2.3		1.6	

Global F/C atomic ratios and F/C computed from C1s region, as well as their ratio, are also presented.

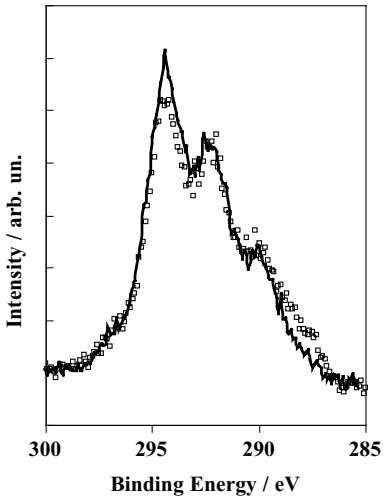

Fig. 8. XPS C1s region for two post-mould fluorinated samples of a mixture of 70% virgin plus 30% recyclate HDPE: one readditivated with Recycloblend^{TM} (0.5% of the recyclate material) (bold line) and another one without any readditivation and washed with cyclohexane to remove any traces of previous additives (empty squares).

overlap with those for fluorinated polymer. Otherwise, if fluorine was largely adsorbed, or intercalated in the carbon black or bound to graphitic sites, other F1s components would develop [13]. Also the global F/C atomic ratio as a function of time, similarly to the procedure for a post-mould fluorinated sample in reference [8], was fitted with a function of the type $F/C = a + b\exp(-t/t_0)$ where t_0 is the characteristic time of degradation. The value obtained for t_0 was 230 min, compared with 250 min for the post-mould fluorinated sample. This is also evidence that the fluorine concentration profile is thinner in the in-line fluorinated sample when compared with the post-mould fluorinated sample.

2.4. Role of the introduction of additives

Mechanical and rheological properties of the mixtures of virgin and recycled HDPE, demand a reintroduction of additives. In this study, the role of that readditivation on the ability of the surface to become fluorinated was also studied.

Fig. 8 shows that the role of additivation is not very large but it may not be zero; the sample with reintroduced additives has a slightly larger atomic percentage of (CF_2)-groups and a smaller percentage of unfluorinated sites.

3. Conclusions

SEM images showed that beyond a fluorine concentration in the gaseous flow $[F_2] = 0.06\%$ (v/v), severe corrosion effects appear, pitting being clearly visible in the surface. The extent of the fluorination was greater for greater temperatures but it seems to attain a plateau around 85 °C. Fluorination degree, measured by global F/C atomic ratio also increases with time attaining saturation at around 20 min.

The *fluorability* does not seem to be affected by the composition virgin/recycled HDPE, as both global F/C and F/C (C1s) are identical within experimental error. Therefore both the chemical composition and the fluorine density profile in depth are identical for all compositions.

Both the value of F/C ratio (global F/C)/(F/C (C1s)) and the characteristic time of degradation show that the in-line fluorinated sample has more intensely fluorinated extreme layers but fluorine density profile in depth is thinner in the in-line fluorinated sample than in the post-mould fluorinated sample. The additives showed a minor role in the ability of the surface to be fluorinated.

4. Experimental

Materials were supplied by Ciba and by Solvay. Samples of a range of mixtures of virgin and recycle high density polyethylene (HDPE) with and without (re)additivation were provided by Ciba. Pure virgin HDPE film was supplied by Solvay. All the samples except one contain carbon black (0.2%, w/w). Samples were supplied under the form of films and/or plaques and were fluorinated and analysed as received. A few samples fluorinated in-line were also supplied. The post-mould fluorination was performed in a home-made fluorination line for use under flow conditions (see Scheme 1).

A commercially available mixture of fluorine (F_2) and nitrogen (N_2) 0.09% (v/v) in F_2, purchased from Air Liquide, was used. The composition of the mixture reaching the reactor was varied by mixing pure nitrogen with the 0.09% (v/v) fluorine mixture through a stainless steel serpentine (diameter = 1/8 in.), lined up with the pipeline. The dimensions of the serpentine were chosen to meet the conditions of a turbulent flow regime in order to improve the mixture. The final gaseous fluorine concentration, $[F_2]$, entering the reactor is determined measuring the pressures and flows from the two gas sources: $[F_2] = [Q_1/(Q_1 + Q_2)] \times [F_2]_0$. Q_1 is the feed flow from the $N_2 + F_2$ line, Q_2 is the feed flow from the N_2 line and $[F_2]_0$ is the concentration of fluorine in the mixture bottle. The pressure reducers, type DLRS and DIRS, used to adjust accurately the pressure of the gases that feed the fluorination line, were supplied by air liquide. The mass flowmeters, with a range of 3–45 l h^{-1} N_2, were Fischer & Porter Mod. D10A6142 Purgemaster, supplied by Tecnilab Portugal. The pressure inside the reactor was measured by an industrial pressure transducer, Mod. P675-2 bar, and displayed in a digital display conditioner type CD420, both furnished by Air Liquide. The pressure sensor placed at the entrance of the roughing pump was a Pirani PVD8 digital vacuum gauge. The fluorination reactor was cylindrical with a height of 5 cm and a radius of 5 cm allowing the fluorination of surfaces with 60 cm^2. By-products, consisting mainly of

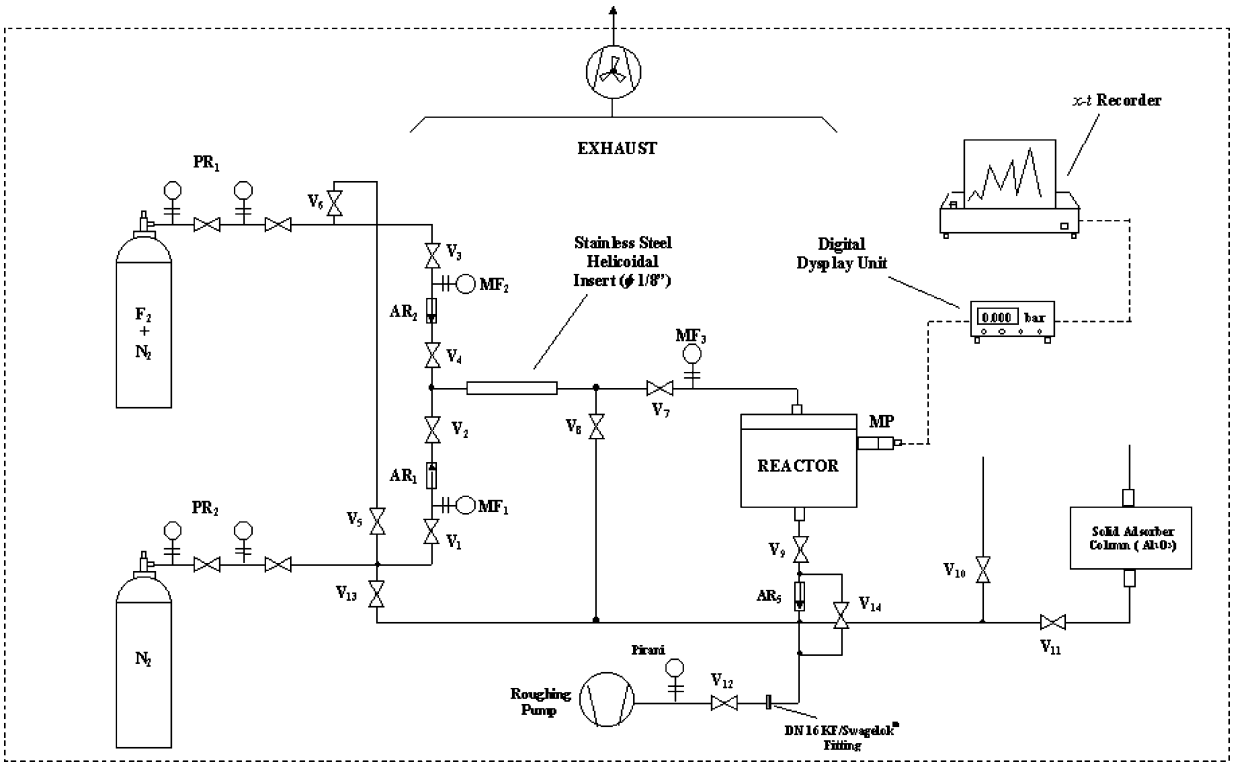

Scheme 1. Fluorination line.

hydrogen fluoride, passed through a purification system before being vented to the atmosphere. The gas waste purification system had two elements: a solid absorber column of activated Al_2O_3 (Alcatel, ref. 068779), followed by an alkaline solution of KOH (Riedel-deHaën, assay: min. 85%). All the valves, the electropolished stainless steel tubes and remaining accessories that compose the apparatus were purchased to Air Liquide.

The X-ray photoelectron spectrometer used was a XSAM800 (KRATOS) model operated in the fixed analyser transmission (FAT) mode. Pass energy of 10 eV, a power of 130 W and the non-monochromatised Mg Kα X-radiation ($hv = 1253.7$ eV) were used. Samples were analysed in ultra high vacuum (UHV), and typical base pressure in the analysis chamber was in the range of 10^{-7} Pa. All sample transfers from the fluorination reactor to the analysis chamber were made under a dry nitrogen atmosphere. Samples were analysed at room temperature, at TOA = 90°–30°. Spectra were collected and stored in 200–300 channels with a step of 0.1 eV, and 60–90 s of acquisition by sweep, using a Sun SPARC Station 4 with Vision software (Kratos). The curve fitting was carried out with a non-linear least-squares algorithm using Voigt profiles. No charge compensation was used. Binding energies were corrected by using a method described elsewhere [8]. For quantification purposes, the sensitivity factors used were: F1s: 1, C1s: 0.25. They were provided by Kratos in the Vision library and checked with high molecular weight PTFE.

The scanning electron microscope was a Hitachi model S2400 SEM of 25 kV. The images presented were obtained with an acceleration voltage of 18 kV and at normal mode (secondary electrons). Due to their insulating character, samples were coated with a ~8 nm thick gold layer, deposited by high vacuum evaporation.

Acknowledgements

We acknowledge the financial support given by EU through the project RECAFUTA, Contract Number BRPR-CT98-0658 in the framework of BRITE-EURAM program. We also acknowledge our partners from Solvay, Dr. J.-M. Yernaux, and CIBA Spezialitätenchemie Lampertheim GmbH, Dr. Rudolf Pfaendner and Dr. Simon Dirk, who provided us all the samples here studied. We also acknowledge all the information given by Solvay about fluorination details.

References

[1] S. Marais, M. Metayer, M. Labbe, J.M. Valleton, S. Alexandre, J.M. Saiter, F. Poncin-Epaillard, Surf. Coat. Technol. 122 (1999) 247–259.

[2] Y. Khairallah, F. Arefi, J. Amouroux, D. Leonard, P. Bertrand, in: M. Strobel, C. Lyons, K.L. Mittal (Eds.), Plasma Surface Modification of Polymers, VSP, 1994, pp. 147–165.

[3] D. Anton, Adv. Mater. 10 (1998) 1197–1296.
[4] A.P. Kharitonov, J. Fluorine Chem. 103 (2000) 123–127.
[5] J. Jagur-Grodzinski, Prog. Polym. Sci. 17 (1992) 361–415.
[6] R.J. Lagow, J.L. Margrave, Progr. Inorg. Chem. 26 (1979) 162–210.
[7] F.J. du Toit, R.D. Sanderson, J. Fluorine Chem. 98 (1999) 107–114, see, for example.
[8] A.M. Ferraria, J.D. Lopes da Silva, A.M. Botelho do Rego, Polymer 44 (2003) 7241–7249.
[9] J.D. Le Roux, D.R. Paul, M.F. Arendt, Y. Yuan, I. Cabasso, J. Memb. Sci. 90 (1994) 37–53.
[10] G. Beamson, D. Briggs, High Resolution XPS of Organic Polymers. The Scienta ESCA300 Database, Wiley, New York, 1992.
[11] R.F. Chiang, P.J. Flory, J. Am. Chem. Soc. 83 (1961) 2857–2862.
[12] J.E. Huheey, Inorganic Chemistry, third ed., Harper International SI Edition, New York, 1983.
[13] A. Tressaud, T. Shirasaki, G. Nansé, E. Papirer, Carbon 40 (2002) 217–220, see, for example and references therein.